THE JOURNAL OF BIOLOGICAL CHEMISTRY
Vol. 278, No. 32, Issue of August 8, pp. 29686–29692, 2003
Printed in U.S.A.

Peptides Induce ATP Hydrolysis at Both Subunits of the Transporter Associated with Antigen Processing*

Received for publication, March 18, 2003, and in revised form, May 13, 2003
Published, JBC Papers in Press, May 30, 2003, DOI 10.1074/jbc.M302757200

Min Chen, Rupert Abele, and Robert Tampé‡

From the Institute of Biochemistry, Biocenter, Goethe-University Frankfurt, Marie-Curie-Strasse 9, D-60439 Frankfurt am Main, Germany

The transporter associated with antigen processing (TAP) plays a key role in the adaptive immune response by pumping antigenic peptides into the endoplasmic reticulum for subsequent loading of major histocompatibility complex class I molecules. TAP is a heterodimer consisting of TAP1 and TAP2. Each subunit is composed of a transmembrane domain and a nucleotide-binding domain, which energizes the peptide transport. To analyze ATP hydrolysis of each subunit we developed a method of trapping 8-azido-nucleotides to TAP in the presence of phosphate transition state analogs followed by photocross-linking, immunoprecipitation, and high resolution SDS-PAGE. Strikingly, trapping of both TAP subunits by beryllium fluoride is peptide-specific. The peptide concentration required for half-maximal trapping is identical for TAP1 and TAP2 and directly correlates with the peptide binding affinity. Only a background level of trapping was observed for low affinity peptides or in the presence of the herpes simplex viral protein ICP47, which specifically blocks peptide binding to TAP. Importantly, the peptide-induced trapped state is reached after ATP hydrolysis and not in a backward reaction of ADP binding and trapping. In the trapped state, TAP can neither bind nor exchange nucleotides, whereas peptide binding is not affected. In summary, these data support the model that peptide binding induces a conformation that triggers ATP hydrolysis in both subunits of the TAP complex within the catalytic cycle.

Cytotoxic T-lymphocytes recognize peptides as a "non-self" signal presented by MHC[1] class I molecules at the cell surface. These antigenic peptides, which are derived from endogenous proteins, are degraded within the proteasomal pathway in the cytosolic compartment. The transporter associated with antigen processing (TAP) translocates these peptides into the ER lumen, where loading of peptides on MHC class I molecules takes place (1). Subsequently, fully assembled MHC·peptide complexes can pass the ER quality control and traffic to the cell surface, where they are inspected by cytotoxic T-lymphocytes.

TAP belongs to the ABC transporter superfamily, whose members share the common structural organization of four domains: two transmembrane domains (TMDs) and two nucleotide-binding domains (NBDs) (2). The TMDs are generally formed by 5–10 transmembrane helices, whereas the NBDs are defined by three consensus motifs: Walker A, Walker B, and C-signature sequences. Functional TAP is a heterodimer consisting of TAP1 and TAP2, each of which contains one N-terminal TMD followed by a C-terminal NBD (3). The transmembrane domains determine the peptide specificity and form a putative translocation pore across the membrane, whereas the nucleotide-binding domains catalyze the ATP hydrolysis and provide the energy for peptide translocation.

TAP binds peptides with a preferential length of 8–16 amino acids (4). Substrate selectivity is determined by the three amino-terminal residues and the carboxyl-terminal residue of the peptide (5). Peptide binding induces a drastic structural reorganization of the TAP complex as shown recently by kinetic and thermodynamic studies (6, 7). This structural rearrangement triggers ATP hydrolysis and peptide transport as deduced from the allosteric coupling between peptide binding and ATP hydrolysis (8).

In addition to being an energy source, nucleotides are important regulatory factors. The release of MHC class I molecules from the loading complex, consisting of TAP1, TAP2, tapasin, and MHC class I molecules, was proposed to be tightly regulated by nucleotide binding (9). Moreover, binding of ATP or ADP stabilizes TAP (10). Deficiency of TAP in ATP binding and hydrolysis was also reported to be related to viral infection: The human cytomegaloviral protein US6 interferes with MHC class I-mediated antigen presentation by blocking ATP binding to TAP, although interacting in the ER lumen with the peptide transporter (11, 12). In contrast, ICP47 from herpes simplex virus inhibits ATP hydrolysis of TAP by blocking peptide binding to TAP (8).

Peptide translocation is strictly dependent on ATP hydrolysis (4, 5, 13). Several groups have recently addressed the function of the two NBDs in the peptide transport process (reviewed in Ref. 14). Exchanging the highly conserved, catalytic active lysine residue of the Walker A site impairs the transport activity strongly. Interestingly, although mutations of this residue in TAP2 fully interrupt peptide transport, TAP1 mutants show still low transport activity, suggesting distinct functions of both subunits during peptide transport (15–17). A functional non-equivalence of the two NBDs has also been reported in studies exchanging the NBDs within the TAP complex. The chimera with switched NBDs has substantial higher transport activity than chimeras with two identical NBDs, indicating that two different NBDs are important for TAP function (18, 19). However, so far it is not clear whether both TAP subunits

* This work was supported by the Deutsche Forschungsgemeinschaft (SFB 628) and the Fonds der Chemischen Industrie. The costs of publication of this article were defrayed in part by the payment of page charges. This article must therefore be hereby marked "*advertisement*" in accordance with 18 U.S.C. Section 1734 solely to indicate this fact.

‡ To whom correspondence should be addressed. Tel.: 49-69-798-29475; Fax: 49-69-798-29495; E-mail: tampe@em.uni-frankfurt.de.

[1] The abbreviations used are: MHC, major histocompatibility complex; ABC, ATP-binding cassette; BeF_x, beryllium fluoride; CFTR, cystic fibrosis transmembrane conductance regulator; ER, endoplasmic reticulum; IP, immunoprecipitation; MALDI-TOF, matrix-assisted laser desorption ionization-time of flight; NBD, nucleotide-binding domain; P-gp, P-glycoprotein; TAP, transporter associated with antigen processing; TMD, transmembrane domain.

catalyze ATP hydrolysis. This question could neither be answered by measuring ATPase activity of TAP, nor could mutagenesis studies clarify this point directly.

In this study, the ATP hydrolysis properties of the two TAP subunits were studied for the first time by photolabeling with 8-azido-[α-^{32}P]ATP combined with BeF_x trapping. It was demonstrated that the trapping reaction reflects the ATP hydrolysis of TAP. Peptides specifically induce BeF_x trapping, whereas the TAP inhibitor ICP47 from herpes simplex virus blocks it. Very importantly, peptide-stimulated nucleotide trapping was found to occur at both subunits. In the BeF_x-trapped state, TAP can neither bind nor exchange nucleotides, whereas peptide binding is not affected. Here, we provide direct evidence that TAP1 and TAP2 hydrolyze ATP within the peptide translocation process.

EXPERIMENTAL PROCEDURES

Material—8-Azido-[α-^{32}P]ATP and 8-azido-[α-^{32}P]ADP were purchased from Affinity Labeling Technologies. Sodium orthovanadate was freshly prepared before use according to the method of Goodno (20). All metal fluorides were prepared before use by mixing metal chloride with sodium fluoride. Peptides used in this study were RRYQKSTEL (R9LQK), RRYQNSTEL, EPGNTWDED (E9D), and a D-isomer of R9LQK (D-R9LQK), in which all residues were exchanged by D-amino acids. In inhibition experiments, the active domain of ICP47 (residue 3–34) was used (21).

Cell Culture and Preparation of Microsomes—Human Burkitt lymphoma cells (Raji cells) were cultured in roller bottles in RPMI 1640 medium (Invitrogen) supplemented with 10% fetal calf serum, 1 mM sodium pyruvate, and 40 units/ml penicillin and streptomycin at 37 °C in 5% CO_2. Sf9 (*Spodoptera frugiperda*) cells were grown in Sf900II medium (Invitrogen) following standard procedures. Infection with the baculovirus encoding human TAP1 and TAP2 was routinely performed with a multiplicity of infection of 3–5 (22). Microsomes were prepared as described previously (22), suspended in phosphate-buffered saline, 1 mM dithiothreitol, pH 7.0, snap frozen in liquid N_2 and stored at −80 °C.

Iodination of Peptides—All peptides were synthesized by solid-phase technique applying conventional Fmoc (*N*-(9-fluorenyl)methoxycarbonyl) chemistry and purified by reversed-phase high performance liquid chromatography. The identity of the peptides was confirmed by MALDI-TOF mass spectrometry. Radiolabeled peptides were prepared as described previously (22) with the following modification. In brief, the reaction was carried out with 1.5 nmol of peptides, 100 μCi of $Na^{125}I$, and 10 μg of chloramine T in a volume of 60 μl. The reaction was stopped by addition of 120 μl of 0.17 mg/ml $Na_2S_2O_5$. Free iodide was removed by Dowex 1X8 (Serva).

Peptide Binding and Transport Assay—Peptide binding to TAP in microsomes was analyzed in AP buffer (phosphate-buffered saline buffer, 5 mM $MgCl_2$, pH 7.0). Microsomes (250 μg of protein) were mixed with ^{125}I-labeled peptide R9LQK in a volume of 150 μl. After 15 min of incubation on ice, 1 ml of AP buffer was added and microsomes were centrifuged at 20,000 × *g* for 8 min. After washing with 500 μl of AP buffer, the radioactivity associated with microsomes was quantified by γ-counting. The amount of unspecific binding was determined in the presence of a 400-fold excess of unlabeled peptide. To analyze peptide transport, microsomes (250 μg of protein) were incubated with 1 μM ^{125}I-labeled RRYQNSTEL, 3 mM ATP, or ADP in 50 μl of AP buffer for 2 min at 32 °C. The reaction was stopped by adding 500 μl of ice-cold AP buffer supplemented with 10 mM EDTA. After centrifugation, the pellets were solubilized in 900 μl of lysis buffer (20 mM Tris, 150 mM NaCl, 5 mM $MgCl_2$, 1% Igepal, pH 7.5) by incubation for 15 min on ice. The insoluble material was removed by centrifugation, and the supernatant was incubated with 60 μl of concanavalin A (ConA)-Sepharose (50%, v/v) for 1 h. After three washing steps, the radioactivity associated with ConA-Sepharose was quantified by γ-counting.

Inhibition of Peptide Transport by BeF_x—To induce the formation of a BeF_x-trapped complex, microsomes (250 μg of protein) were preincubated with 3 mM ATP, 5 mM BeF_x ($BeCl_2$:NaF = 1:10 mol/mol), and 1 μM R9LQK in 50 μl of transport buffer (20 mM HEPES, 140 mM NaCl, 2 mM $MgCl_2$, 5 mM NaN_3, 1 mM ouabain, 0.1 mM EGTA, 15% glycerol, pH 7.5) for 15 min at 27 °C. Subsequently, free ligands were removed by washing with 1 ml of transport buffer. Before use, microsomes were resuspended in 50 μl of transport buffer containing 3 mM ATP.

Photolabeling of TAP with 8-Azido-[α-^{32}P]ATP—Microsomes were suspended in 25 μl of transport buffer containing 1 μM 8-azido-[α-^{32}P]ATP. After 5-min incubation at indicated temperature, samples were irradiated with UV light for 5 min on ice. 500 μl of ice-cold IP lysis buffer (20 mM Tris, 150 mM NaCl, 1% Igepal, pH 7.5) was added. Subsequently samples were immunoprecipitated (see below) and analyzed by SDS-PAGE (11%). Gels were dried and exposed to Kodak BIOMAX™ MS films with an intensifying screen at −80 °C.

Trapping of the TAP Complex by ATPase Inhibitors—Microsomes were incubated in 25 μl of transport buffer containing 2 μM 8-azido-[α-^{32}P]ATP and 0.5 mM ATPase inhibitors (orthovanadate, BeF_x, AlF_x, or ScF_x) in the presence or absence of peptides for 15 min at 27 °C. In this assay, all metal fluorides were prepared by mixing metal chloride and sodium fluoride in a molar ratio of 1 to 100. The reaction was stopped by addition of 1 ml of ice-cold washing buffer (transport buffer containing 10 mM ATP and 0.5 mM ATPase inhibitors). Samples were incubated for 15 min on ice. After centrifugation at 20,000 × *g*, pellets were resuspended in 50 μl of washing buffer. Finally, samples were irradiated with UV light for 5 min and then subjected to immunoprecipitation (see below). To determine the peptide concentration at which half-maximal trapping occurs (EC_{50}), the intensities of photolabeled TAP (*I*) were quantified and fitted by Equation 1.

$$I/I_{max} = [\text{peptide}]/(EC_{50} + [\text{peptide}]) \quad \text{(Eq. 1)}$$

Immunoprecipitation—After photolabeling, TAP was immunoprecipitated either as a complex or as disassembled TAP1 and TAP2 subunits. These two methods differ in the solubilization procedure. In the former case, microsomes were solubilized in 0.9 ml of IP lysis buffer for 15 min on ice. In the latter case, microsomes were solubilized in 200 μl of IP lysis buffer for 15 min on ice. To disassemble the TAP complex, SDS was added to a final concentration of 0.5%, and incubation was continued for 15 min at 37 °C. Finally, 700 μl of ice-cold IP lysis buffer was added. In both methods, samples were centrifuged at 20,000 × *g* for 8 min to remove insoluble material after solubilization. Antibodies were added to the supernatant and incubated for 2 h on ice. 50 μl of 50% (v/v) protein A/G-agarose Fast Flow (Sigma) were added, and incubation was continued for 2 h at 4 °C. After washing three times with 1 ml of ice-cold IP washing buffer (20 mM Tris, 150 mM NaCl, 0.1% Igepal, pH 7.5), proteins were eluted with SDS sample buffer and applied to SDS-PAGE (11%). Antibodies used were monoclonal antibody 148.3 (anti-TAP1), rabbit antiserum 1p2 (anti-TAP1), and 2p4 (anti-TAP2). The BeF_x-trapped TAP complex was immunoprecipitated by a combination of polyclonal 1p2 and 2p4. Polyclonal antibodies 1p2 and 2p4 were raised against the peptide epitopes ETEFFQQNQTGNIMSR (TAP1) and VGAAEKVFSYMDRQPN (TAP2) according to Nijenhuis and Hämmerling (23).

RESULTS

8-Azido-ATP Energizes Peptide Transport as Efficiently as ATP—8-Azido-ATP has been used to study the characteristics of binding and/or hydrolysis of ABC transporters such as P-gp, CFTR, and sulfonylurea receptor 1 (SUR1) (24–28). Before using 8-azido-ATP to probe ATP hydrolysis by TAP, we determined whether this ATP-analog drives peptide transport. Therefore, peptide transport quantified by the amount of glycosylated, radiolabeled peptide was analyzed in the presence of ATP or 8-azido-ATP. The accumulation of peptides in microsomes increases linearly within the first 2 min (data not shown). The initial transport rates were determined at increasing ATP or 8-azido-ATP concentrations and fitted with Michaelis-Menten kinetics (Fig. 1). The apparent K_m values for both nucleotides show only a slight difference, which are 197 ± 35 μM for ATP and 103 ± 24 μM for 8-azido-ATP, whereas the V_{max} for both nucleotides is equal. From these results, we conclude that 8-azido-ATP support peptide translocation as efficiently as ATP and modification of the C_8 position of the adenine base does not change the properties of the nucleotide during the catalytic cycle.

8-Azido-ATP Binds Specifically to TAP1 and TAP2—Next, we examined the nucleotide binding property of TAP by 8-azido-[α-^{32}P]ATP photocross-linking. After immunoprecipitation, TAP1 and TAP2 (apparent molecular mass, 71 and 75 kDa) were separated by high resolution SDS-PAGE (Fig. 2). The identity of the two TAP subunits was confirmed by immu-

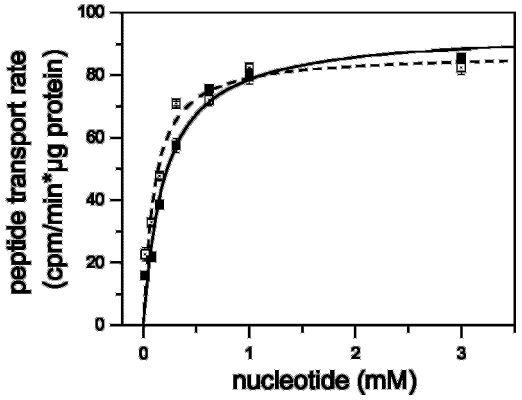

FIG. 1. **TAP-dependent peptide transport in the presence of ATP and 8-azido-ATP.** Microsomes prepared from insect cells infected with recombinant baculovirus encoding human TAP1 and TAP2 were incubated with 1 μM radiolabeled RRYQNSTEL at various concentrations of ATP (*filled symbols*) or 8-azido-ATP (*open symbols*) at 32 °C for 2 min. Glycosylated peptides were recovered by ConA-Sepharose, and the radioactivity was quantified by using γ-counting. The data were fitted with the Michaelis-Menten equation leading to a K_m value of 197 ± 35 μM for ATP (*solid*) and 103 ± 24 μM for 8-azido-ATP (*dashed line*). Data points and errors were derived from triplicate measurements.

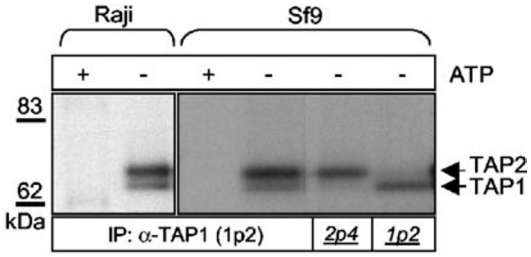

FIG. 2. **8-Azido-[α-^{32}P]ATP photocross-linking of TAP.** Microsome preparations (50 μg of protein) from Raji cells or Sf9 insect cells infected with baculovirus encoding human TAP1/TAP2 were incubated with 1 μM 8-azido-[α-^{32}P]ATP in the presence or absence of 1 mM ATP on ice. Proteins were photolabeled by UV irradiation for 5 min. The two subunits were either co-immunoprecipitated as an intact heterodimeric complex via TAP1-specific antiserum (1p2) or as dissociated subunits via TAP1- or TAP2-specific antibodies (*1p2* and *2p4*). The immunoprecipitated products were analyzed by SDS-PAGE (11%) and visualized by autoradiography.

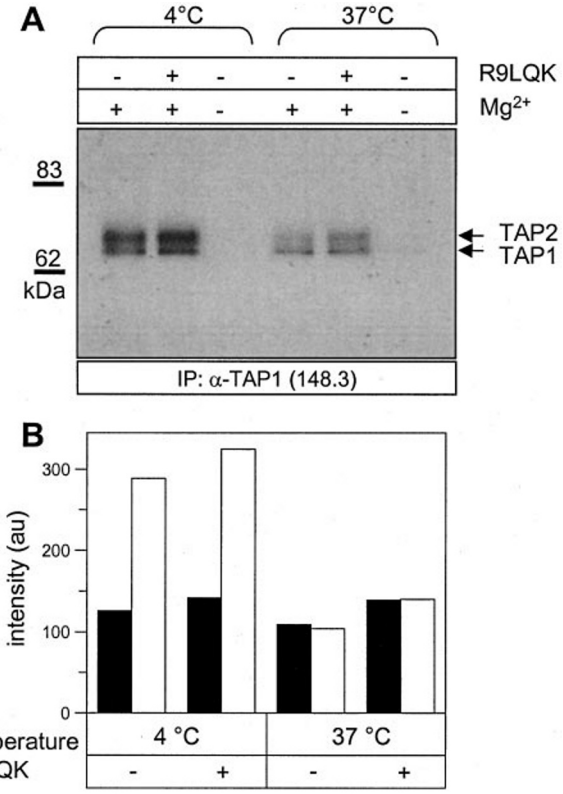

FIG. 3. **Effect of Mg^{2+} and temperature on 8-azido-[α-^{32}P]ATP photocross-linking.** *A*, microsomes (100 μg of protein) prepared from Raji cells were incubated with 1 μM 8-azido-[α-^{32}P]ATP in the presence or absence of 1 mM $MgCl_2$ or 1 μM R9LQK for 5 min at 4 °C or 37 °C. Samples at 37 °C were transferred on ice, and all probes were immediately subjected to UV irradiation. The TAP complex was precipitated via anti-TAP1 monoclonal antibody 148.3, separated by SDS-PAGE (11%), and analyzed by autoradiography. *B*, to compare the slight increase in labeling efficiency in the presence of peptide the corresponding TAP1 (*filled bars*) and TAP2 (*open bars*), bands were densitometrically analyzed, and intensities are shown as a histogram.

noprecipitation of disassembled TAP1 and TAP2 subunits. The photocross-linking is specific, because it was inhibited by 1 mM ATP, demonstrating its specificity. Interestingly, even after immunoprecipitation of the TAP complex with an anti-TAP1 antibody, TAP2 shows stronger photolabeling than TAP1. This preferential labeling of TAP2 was observed both for TAP derived from Raji cells and for TAP expressed in insect cells lacking factors of the MHC loading complex. These results demonstrate that both subunits bind 8-azido-ATP specifically, and TAP2 is photolabeled more efficiently than TAP1.

8-Azido-ATP Binding to TAP1 and TAP2 Is Magnesium- and Temperature-dependent—Magnesium is well known to be required for ATP hydrolysis by most ATPases. It has also been shown that Mg^{2+} can have different effects on ATP binding to two subunits of an ABC transporter (29). Therefore, we examined the influence of magnesium on 8-azido-[α-^{32}P]ATP photolabeling of the TAP complex. No photolabeling of TAP1 and TAP2 was observed in the absence of magnesium either at 4 °C or 37 °C, indicating that ATP binding to both TAP subunits is magnesium-dependent (Fig. 3*A*). Nucleotide binding to the TAP complex is temperature-dependent. At 4 °C, photolabeling preferentially occurred at TAP2. However, at 37 °C, TAP1 and TAP2 are equally labeled, and the photolabeling of both subunits is weaker than at 4 °C. Peptides slightly stimulate the labeling of both subunits (Fig. 3*B*).

Phosphate Analogs Trap ADP in TAP1 and TAP2—The contribution of each NBD to the ATPase activity of TAP cannot be directly analyzed by measuring the steady-state release of inorganic phosphate. ATPase inhibitors, such as orthovanadate, BeF_x, AlF_x, or ScF_x, are useful tools to elucidate the mechanism of ATP hydrolysis by forming a stable Mg·ADP·inhibitor complex after ATP hydrolysis and phosphate release arresting the enzyme in the catalytic cycle (30–33). Therefore, TAP-containing microsomes were incubated with 8-azido-[α-^{32}P]ATP in the presence of different ATPase inhibitors at 37 °C to test their ability to form a trapped Mg·ADP·inhibitor·TAP complex. After trapping, weakly bound nucleotides were removed by washing the microsomes. Photolabeling of TAP1 and TAP2 was observed in the presence of all three metal fluorides, whereas very weak signals were found in the presence of vanadate (Fig. 4). No photolabeling was observed in the absence of trapping reagents. Microsomes derived from insect cells infected with baculovirus wild-type also showed no photolabeling. The trapping reaction was peptide-specific, and this is investigated in detail below. These data demonstrate that metal fluorides form a trapped state with ADP within the NBD of TAP1 and TAP2. This state is very stable, because trapped ADP cannot be competed out even by a 1000-fold excess of ATP. In all cases stronger labeling of TAP1 than TAP2 was observed. In summary, the phosphate analogs trap ADP in TAP with the following efficiencies: $BeF_x > ScF_x > AlF_x \gg V_i$.

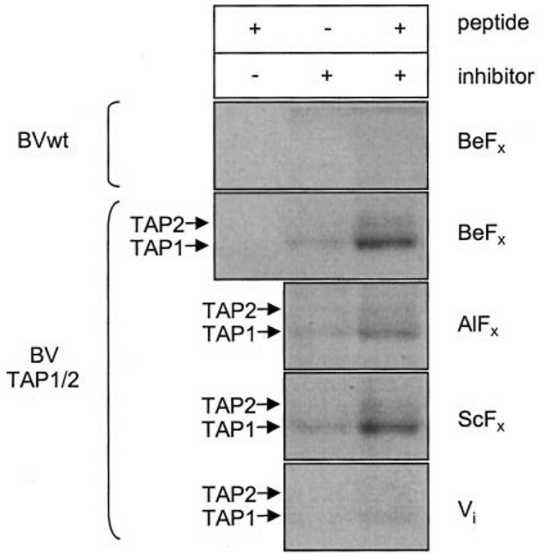

FIG. 4. **Analysis of ATPase inhibitors of TAP.** Microsomes (50 μg of protein) from insect cells infected with baculovirus (*BV*) encoding human TAP1/2 or wild type baculovirus were incubated with 2 μM 8-azido-[α-^{32}P]ATP either in the absence or presence of 0.5 mM of different inhibitors (BeF$_x$, AlF$_x$, ScF$_x$, or orthovanadate) and 1 μM peptide R9LQK for 15 min at 27 °C. After washing and UV-photocrosslinking, samples were subjected to SDS-PAGE (11%) and visualized by autoradiography.

Peptides Induce the Formation of a Trapped Intermediate State of TAP1 and TAP2—It has been recently demonstrated that ATP hydrolysis is coupled to peptide binding and transport (8). However, it remains unclear whether TAP1 or TAP2, or both subunits are involved in ATP hydrolysis. Here, we investigated the effect of various peptides on BeF$_x$ trapping of Mg-8-azido-[α-^{32}P]ADP by incubating TAP with 8-azido-[α-^{32}P]ATP under hydrolyzing conditions. Both subunits were strongly labeled in the presence of the high affinity peptide R9LQK and BeF$_x$ (Fig. 5*A*). A very weak labeling for TAP1 and TAP2 was observed in the presence of the herpes simplex virus protein ICP47, which specifically inhibits peptide binding and thus prevents the peptide-stimulated ATPase activity of TAP (8, 34). Furthermore, a weak labeling of TAP was found in the presence of the low affinity peptides (K_D > 1 mM), E9D and D-R9LQK. In the absence of BeF$_x$, no labeling of TAP was detected even when high affinity peptides are present. To analyze the peptide-induced formation of a trapped intermediate quantitatively, BeF$_x$ trapping was performed with increasing concentrations of R9LQK. Photolabeling of both TAP subunits was enhanced in a concentration-dependent manner (Fig. 5*B*). The EC$_{50}$ values (peptide concentration required to achieve half-maximal trapping) for TAP1 and TAP2 are very similar with 16 nM and 18 nM, respectively (Fig. 5*C*). These values are in good agreement with the affinity constant of fluorescein-labeled R9LQK (12 nM) measured under equilibrium binding condition (6). Interestingly, under all trapping conditions, TAP1 was preferentially labeled. Taken together, these data demonstrate that peptides specifically induce BeF$_x$ trapping of both TAP subunits.

BeF$_x$-trapping Reflects ATP Hydrolysis—Peptide-induced BeF$_x$ trapping of TAP might be due to two different mechanisms: (i) BeF$_x$ substitutes the released phosphate immediately after ATP hydrolysis, forming a stable Mg·ADP·BeF$_x$ complex within the NBD (forward reaction); (ii) ATP is hydrolyzed by ATPases present in the microsomal preparation. Trapping is initiated by binding of MgADP to TAP, followed by association of BeF$_x$ and by formation of a stable NBD·Mg·ADP·BeF$_x$ complex (backward reaction). To distinguish between the two pathways, we compared BeF$_x$ trapping in the presence of the 8-azido-[α-^{32}P]ATP and 8-azido-[α-^{32}P]ADP. The concentration as well as the radioactivity of the two nucleotides was kept identical to allow direct comparison of the signal intensities. The high affinity peptide R9LQK strongly stimulates the trapping of TAP with 8-azido-[α-^{32}P]ATP (Fig. 6). Moreover, in the case of 8-azido-[α-^{32}P]ADP, the trapping efficiency of TAP is

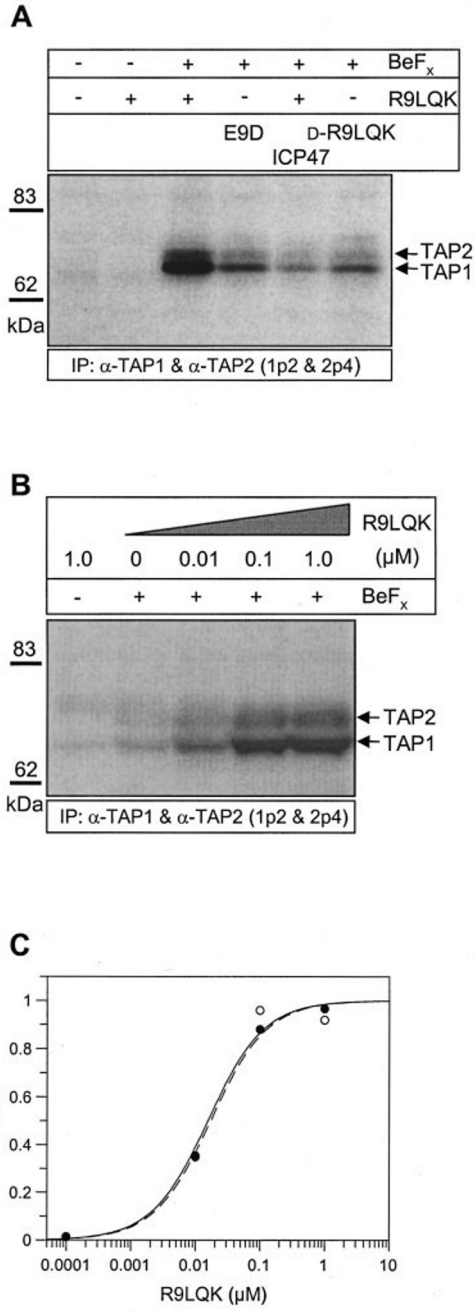

FIG. 5. **Peptide-induced BeF$_x$ trapping of TAP1 and TAP2.** Trapping of TAP was performed by incubating Raji microsomes (100 μg of protein) with 2 μM 8-azido-[α-^{32}P]ATP in the presence or absence of 0.5 mM BeF$_x$ and/or 1 μM of different peptides (*A*) or increasing R9LQK concentration (*B*) following the procedure described under "Experimental Procedures." To investigate the effect of the viral inhibitor ICP47, microsomes were incubated with 20 μM ICP47. The TAP complex was immunoprecipitated by polyclonal antibodies 1p2 and 2p4 and analyzed by SDS-PAGE (11%) followed by autoradiography. To determine the EC$_{50}$ values for peptide-induced trapping, the photolabeling of TAP1 and TAP2 was quantified. The background-corrected intensities were plotted against concentration of R9LQK and fitted with Equation 1. The EC$_{50}$ values for trapping of TAP1 (*open circle* and *dashed line*) and TAP2 (*close circles* and *solid line*) are 18 and 16 nM, respectively (*C*).

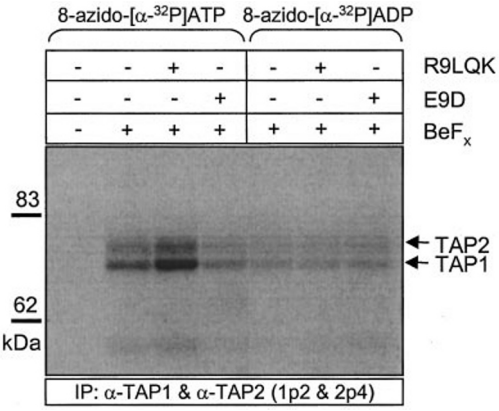

FIG. 6. **Comparison of 8-azido-ATP and 8-azido-ADP trapping with BeF_x.** Trapping of TAP was performed by incubating Raji microsomes (100 μg) with 2 μM 8-azido-[α-^{32}P]ATP (5 μCi) or 2 μM 8-azido-[α-^{32}P]ADP (5 μCi) with or without 0.5 mM BeF_x and 1 μM R9LQK or E9D for 15 min at 27 °C (for details see "Experimental Procedures"). The TAP complex was immunoprecipitated via antibodies 1p2 and 2p4, separated by SDS-PAGE (11%), and visualized by autoradiography.

not peptide-dependent and lower than in the presence of 8-azido-[α-^{32}P]ATP. Therefore, we conclude that efficient BeF_x trapping of TAP occurs only after ATP hydrolysis and that the peptide-induced BeF_x trapping directly reflects ATP hydrolysis during the catalytic cycle of TAP.

Peptide Transport and Nucleotide Binding, but Not Peptide Binding, Is Inhibited in the BeF_x-trapped State of TAP—To characterize the BeF_x-trapped state of TAP in more detail, peptide and nucleotide binding as well as peptide transport of trapped TAP were analyzed. After incubation of microsomes with BeF_x and ATP for 15 min, peptide transport via TAP was reduced to 20% (Fig. 7*A*). Longer incubation with BeF_x blocked the TAP transport activity completely. However, longer incubation time also impaired TAP function. The stability of the trapping state was examined by monitoring the recovery of peptide transport over time. For this purpose, free BeF_x was removed to facilitate the dissociation of TAP·Mg·ADP·BeF_x complex. It was observed that even after incubation for 45 min on ice, TAP remains in an inhibited state. Longer recovery times were not analyzed, because TAP started to loose activity even at 4 °C. Next, we studied the BeF_x-trapped TAP complex with respect to nucleotide and peptide binding. Fig. 7*B* shows that pretreatment of TAP with BeF_x and ATP inhibits the photolabeling with 8-azido-[α-^{32}P]ATP and 8-azido-[α-^{32}P]ADP, demonstrating that the trapped state of TAP can neither bind nor exchange added nucleotides. The weaker photolabeling signal of TAP preincubated with ATP compared with that without ATP results from incomplete dissociation of ATP during the washing step. In contrast to nucleotide binding, BeF_x trapping does not affect peptide binding (Fig 7*C*). At half-maximal and saturating peptide concentrations, the amount of peptides bound to the trapped and non-trapped state is equal. These data demonstrate that neither the affinity nor the overall amount of the peptide binding sites was altered. In addition, the same results were obtained when AlF_x and ScF_x were used for trapping (data not shown). Taken together, BeF_x inhibits peptide translocation by trapping TAP in a stable intermediate state to which added nucleotides cannot bind. Importantly, peptide binding to TAP is not affected in this trapped state.

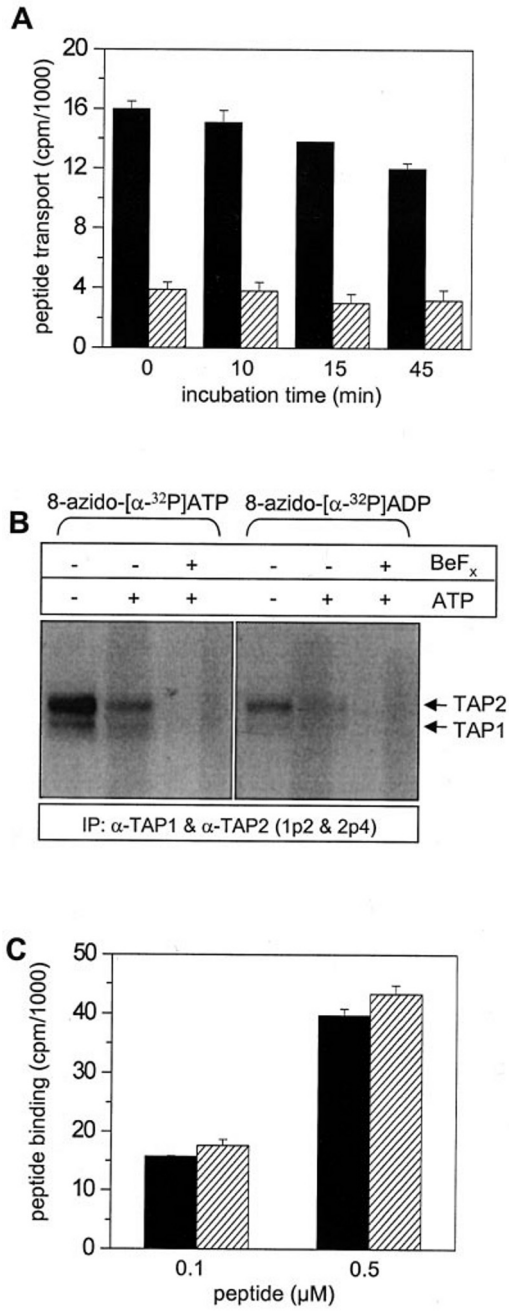

FIG. 7. **Characterization of the BeF_x-trapped TAP complex.** *A*, stability of the BeF_x-trapped TAP complex. Raji microsomes (250 μg of protein) were incubated with 1 μM R9LQK, 3 mM ATP in the absence (*solid bar*) or presence (*hatched bar*) of 5 mM BeF_x at 27 °C for 15 min. Subsequently, free and un-trapped nucleotides and peptides were removed by washing, and microsomes were resuspended in transport buffer containing 3 mM ATP and incubated on ice. After different time periods, peptide transport was initiated by adding 1 μM radiolabeled RRYQNSTEL and immediately transferring samples to 32 °C for 2 min. Translocated peptides were recovered on ConA beads and quantified by γ-counting. *B*, binding of nucleotides to the BeF_x-trapped TAP complex. Raji microsomes (100 μg of proteins) were incubated with 1 μM R9LQK in the presence or absence of 3 mM ATP and/or 5 mM BeF_x (Be:F = 1:10 mol/mol) at 27 °C for 15 min. After washing the microsomes to remove all free and loosely bound nucleotide and peptide, microsomes were incubated with 1 μM 8-azido-[α-^{32}P]ATP or 8-azido-[α-^{32}P]ADP for 5 min on ice, followed by UV irradiation. TAP1 and TAP2 were co-immunoprecipitated by a combination of polyclonal antibodies 1p2 and 2p4. *C*, peptide binding to the BeF_x-trapped TAP complex. Raji microsomes (250 μg of proteins) were incubated with 3 mM ATP and 1 μM R9LQK in the absence (*solid bar*) or presence (*hatched bar*) of 5 mM BeF_x (Be:F = 1:10 mol/mol) at 27 °C for 15 min. After washing, peptide binding of radiolabeled R9LQK was determined as described under "Experimental Procedures."

DISCUSSION

In the last decade, major advances have been made in the study of the mechanism of peptide transport by TAP: (i) the peptide specificity and the peptide binding mechanism of TAP

were deciphered in detail (5–7); (ii) the importance of the nucleotide-binding domains of TAP for peptide transport was shown by mutation analysis (9, 15–17, 35); and (iii) the allosteric coupling between peptide binding, ATP hydrolysis and peptide transport was observed with reconstituted TAP (8). However, the contribution of each subunit in the TAP complex to ATP hydrolysis was not characterized up to now. By using the technique of BeF_x trapping of 8-azido-[α-^{32}P]ATP followed by photolabeling, immunoprecipitation and separation of the TAP subunits by high resolution SDS-PAGE, we analyzed the ATPase activity of TAP1 and TAP2 for the first time. Using the ATPase inhibitor BeF_x formation of a stable complex consisting of Mg·ADP·BeF_x bound to NBD was achieved. For myosin, a trapping of Mg·ADP by BeF_x longer than 3 days is reported (36). Restricted by the instability of TAP, we showed that the trapped TAP complex is at least stable for 45 min.

We showed that BeF_x trapping of TAP is peptide-specific. High affinity peptides induced nucleotide trapping of both subunits of TAP in a concentration-dependent manner. This reflects the peptide-stimulated ATPase activity of the TAP complex reported in earlier work (8). Although these previous results demonstrated that peptide binding correlates with ATP hydrolysis, we now provide evidence that ATP hydrolysis at both subunits is induced by peptides with an EC_{50} corresponding to the affinity of the peptide. These observations are in line with the model that peptide binding to TAP is responsible for a dramatic structural rearrangement (7) that triggers ATP hydrolysis by the NBDs of TAP1 and TAP2 resulting in peptide translocation. The low amount of trapping in the absence of peptide or in the presence of low affinity peptides could result from a low intrinsic ATPase activity of TAP. However, in the presence of US6, which blocks ATP binding, no reduction of background ATPase activity could be observed excluding an intrinsic ATPase activity of TAP (12). Therefore, background trapping probably caused a backward reaction, in which 8-azido-[α-^{32}P]ADP produced by other ATPases is bound and trapped at TAP. This point is supported by the observation that trapping of 8-azido-ADP results in the same labeling efficiency of TAP as with 8-azido-ATP in the presence of the viral inhibitor ICP47, which blocks peptide binding to TAP. In addition, endogenous peptides produced by proteases present in the microsomal preparation might also slightly stimulate BeF_x trapping of TAP.

The trapped state can be formed independently of ATP hydrolysis, as indicated in the studies of P-gp, MRP6, and myosin, which were trapped from an ADP binding state (backward reaction) by vanadate or metal fluorides in the absence of ATP hydrolysis (37–39). With low efficiency, BeF_x also traps TAP from an ADP binding state. Importantly, however, the trapping of 8-azido-ADP is not affected by peptides. These observations are in line with studies on P-gp showing that trapping without ATP hydrolysis is energetically less favorable. Substrate-induced trapping of P-gp is only achieved after ATP hydrolysis and is strongly inhibited in presence of ADP (37, 40).

Surprisingly, the trapping efficiency of TAP by orthovanadate is very low in comparison to BeF_x. Similar results are reported for MRP6, where BeF_x traps ADP very efficiently and vanadate could only trap ADP in presence of Ni^{2+} (39). The trapping efficiencies of phosphate analogs can be discussed by comparing the x-ray structures of myosin in complex with Mg·ADP·BeF_4^{2-}, Mg·ADP·AlF_4^-, and Mg·ADP·V_i (31, 41). The V_i/AlF_4^--inhibited complexes reflecting most probably the myosin·Mg·ADP-P_i transition state were very similar, and the distance between Al/V and the bridging oxygen of the β-phosphate group of ADP was 2.0 Å for AlF_4^- and 2.1 Å for V_i. However, in the BeF_x-trapped state, which resembles the ground state before ATP hydrolysis occurs, the distance between Be and the bridging oxygen was only 1.6 Å. Based on this knowledge, the differences in trapping Mg·ADP to TAP were probably caused by small structural differences in the ATP-binding pocket, in which Mg·ADP·BeF_x fits well forming a stable complex.

The crystal structure of the monomeric NBD of TAP1 is highly similar to other NBDs of ABC transporters (42). The structure of the E171Q mutant of MJ0796 and the orientation of the NBDs of the vitamin B_{12}-transporter BtuCD resemble the Rad50 dimer in which the ATP binding pocket is formed from the Walker A and B sequences of one subunit and the C-loop of the other subunit (43–45). We propose that this dimer structure represents a physiologic intermediate that occurs transiently during the transport cycle when ATP is bound. Therefore, in the trapped state, the NBDs of TAP should be closely associated resembling the structure of the NBD dimer. This could explain that, in the trapped state, TAP neither binds nor exchanges nucleotides. This observation is in agreement with soluble expressed NBDs of the structural and functional TAP homolog Mdl1p, a homodimeric ABC peptide transporter located in the inner mitochondrial membrane. The NBDs of Mdl1p form stable BeF_x-trapped dimers after ATP hydrolysis. The BeF_x-trapped NBD dimer contains two ADP molecules, which cannot be exchanged by nucleotides (57).

With the structure of the NBD dimer in mind, it is surprising that both TAP subunits show different labeling efficiency. At 4 °C, TAP2 shows stronger 8-azido-ATP photolabeling than TAP1. This difference reflects the 2-fold higher affinity of TAP2 (2.7 μM) for 8-azido-ATP than TAP1 (4.6 μM) as reported recently (46). However, in the BeF_x-trapped state, TAP1 is more strongly photocross-linked than TAP2. The possibility that trapped 8-azido-ADP bound to the Walker A site of TAP2 photoreacts with the C-loop of TAP1 is very unlikely, because it was shown that trapped 8-azido-[α-^{32}P]ADP is photocross-linked to a tyrosine residue of P-gp, which is highly conserved throughout ABC transporters and forms π-π interactions with the adenine ring (42, 43, 47, 48). Furthermore, it is very unlikely that the different signals of trapped nucleotide arise from different ATPase activities of both subunits during peptide transport. In this case TAP1 should hydrolyze more ATP than TAP2, which is in contrast to the cooperativity between both NBDs as reported for other ABC transporter (49–51). Therefore, kinetic or structural differences between both ATP binding sites must likely be the reason for the different labeling efficiencies. One possibility is that two ATPs are hydrolyzed within the dimer during peptide transport; TAP2 might release ADP faster than TAP1 resulting in a lower trapping yield. Another possibility is that the two nucleotide binding sites differ slightly resulting in a more stable Mg·ADP·BeF_x complex for TAP1 than for TAP2.

In this report, we demonstrate that BeF_x traps ADP in TAP1 and TAP2 after peptide-stimulated ATP hydrolysis. However, we could not decide whether one or two nucleotides are fixed within the heterodimeric TAP complex at the same time. Principally, two possibilities are found for the trapped state of ABC transporters: (i) both subunits have tightly bound nucleotides in the trapped state, or (ii) only one nucleotide is associated with the ABC transporter after trapping. In the case of the chloride channel CFTR, an occlusion of NBD1 with 8-azido-[α-^{32}P]ATP is observed that can be enhanced under vanadate trapping conditions that also strongly traps 8-azido-[α-^{32}P]ADP to NBD2 (52). Consequently, in the trapped state, one ADP and one ATP are bound to NBD2 and NBD1 of CFTR, respectively. In contrast, only one ADP is bound to P-gp and the maltose permease in the vanadate-trapped state (53, 54). These

differences in trapping are also reflected in the effect of mutations of the highly conserved lysine in Walker A sequence. Mutation of any NBD of the classic ABC transporters TAP, P-gp, and maltose permease has severe effects on transport or ATPase activity, whereas the same mutation in NBD1 of CFTR does not inhibit significantly the gating (9, 15–17, 35).

A high and low affinity substrate-binding site has been proposed for several drug ABC transporters during the transport process (55, 56). Interestingly, the amount of peptide binding sites and the peptide affinity of TAP are not altered in the BeF_x-trapped intermediate. These data suggest that the peptide has already been translocated across the membrane.

In summary, we provide direct evidence that both NBDs of the TAP complex are active in ATP hydrolysis during the peptide transport process. In line with previous studies, the asymmetric pattern of photolabeling under BeF_x-trapping conditions indicates the distinctive properties of TAP1 and TAP2 with respect to ATP binding and hydrolysis (9, 15–17, 35). Combining the newly established BeF_x trapping of TAP with mutations influencing ATP hydrolysis or peptide transport, the exact role of the two NBDs in TAP function can be addressed.

Acknowledgments—We thank Stanislav Gorbulev and Eva Janas for helpful discussions. We are grateful to Eckhard Linker for his excellent technical assistance. We also thank Hans Bäumert and Chris van der Does for comments on the manuscript.

REFERENCES

1. Pamer, E., and Cresswell, P. (1998) *Annu. Rev. Immunol.* **16,** 323–358
2. Higgins, C. F. (1992) *Annu. Rev. Cell Biol.* **8,** 67–113
3. Abele, R., and Tampé, R. (1999) *Biochim. Biophys. Acta* **1461,** 405–419
4. van Endert, P. M., Tampé, R., Meyer, T. H., Tisch, R., Bach, J. F., and McDevitt, H. O. (1994) *Immunity* **1,** 491–500
5. Uebel, S., Kraas, W., Kienle, S., Wiesmüller, K. H., Jung, G., and Tampé, R. (1997) *Proc. Natl. Acad. Sci. U. S. A.* **94,** 8976–8981
6. Neumann, L., and Tampé, R. (1999) *J. Mol. Biol.* **294,** 1203–1213
7. Neumann, L., Abele, R., and Tampé, R. (2002) *J. Mol. Biol.* **324,** 965–973
8. Gorbulev, S., Abele, R., and Tampé, R. (2001) *Proc. Natl. Acad. Sci. U. S. A.* **98,** 3732–3737
9. Knittler, M. R., Alberts, P., Deverson, E. V., and Howard, J. C. (1999) *Curr. Biol.* **9,** 999–1008
10. van Endert, P. M. (1999) *J. Biol. Chem.* **274,** 14632–14638
11. Hewitt, E. W., Gupta, S. S., and Lehner, P. J. (2001) *EMBO J.* **20,** 387–396
12. Kyritsis, C., Gorbulev, S., Hutschenreiter, S., Pawlitschko, K., Abele, R., and Tampé, R. (2001) *J. Biol. Chem.* **276,** 48031–48039
13. Neefjes, J. J., Momburg, F., and Hammerling, G. J. (1993) *Science* **261,** 769–771
14. van Endert, P. M., Saveanu, L., Hewitt, E. W., and Lehner, P. (2002) *Trends Biochem. Sci.* **27,** 454–461
15. Karttunen, J. T., Lehner, P. J., Gupta, S. S., Hewitt, E. W., and Cresswell, P. (2001) *Proc. Natl. Acad. Sci. U. S. A.* **98,** 7431–7436
16. Lapinski, P. E., Neubig, R. R., and Raghavan, M. (2001) *J. Biol. Chem.* **276,** 7526–7533
17. Saveanu, L., Daniel, S., and van Endert, P. M. (2001) *J. Biol. Chem.* **276,** 22107–22113
18. Arora, S., Lapinski, P. E., and Raghavan, M. (2001) *Proc. Natl. Acad. Sci. U. S. A.* **98,** 7241–7246
19. Daumke, O., and Knittler, M. R. (2001) *Eur. J. Biochem.* **268,** 4776–4786
20. Goodno, C. C. (1982) *Methods Enzymol.* **85,** 116–123
21. Neumann, L., Kraas, W., Uebel, S., Jung, G., and Tampé, R. (1997) *J. Mol. Biol.* **272,** 484–492
22. Meyer, T. H., van Endert, P. M., Uebel, S., Ehring, B., and Tampé, R. (1994) *FEBS Lett.* **351,** 443–447
23. Nijenhuis, M., and Hämmerling, G. J. (1996) *J. Immunol.* **157,** 5467–5477
24. Szabo, K., Welker, E., Bakos, Muller, M., Roninson, I., Varadi, A., and Sarkadi, B. (1998) *J. Biol. Chem.* **273,** 10132–10138
25. Urbatsch, I. L., Sankaran, B., Bhagat, S., and Senior, A. E. (1995) *J. Biol. Chem.* **270,** 26956–26961
26. Hrycyna, C. A., Ramachandra, M., Ambudkar, S. V., Ko, Y. H., Pedersen, P. L., Pastan, I., and Gottesman, M. M. (1998) *J. Biol. Chem.* **273,** 16631–16634
27. Takada, Y., Yamada, K., Taguchi, Y., Kino, K., Matsuo, M., Tucker, S. J., Komano, T., Amachi, T., and Ueda, K. (1998) *Biochim. Biophys. Acta* **1373,** 131–136
28. Ueda, K., Komine, J., Matsuo, M., Seino, S., and Amachi, T. (1999) *Proc. Natl. Acad. Sci. U. S. A.* **96,** 1268–1272
29. Matsuo, M., Kioka, N., Amachi, T., and Ueda, K. (1999) *J. Biol. Chem.* **274,** 37479–37482
30. Urbatsch, I. L., Sankaran, B., Weber, J., and Senior, A. E. (1995) *J. Biol. Chem.* **270,** 19383–19390
31. Smith, C. A., and Rayment, I. (1996) *Biochemistry* **35,** 5404–5417
32. Park, S., Ajtai, K., and Burghardt, T. P. (1999) *Biochim. Biophys. Acta* **1430,** 127–140
33. Wittinghofer, A. (1997) *Curr. Biol.* **7,** R682–R685
34. Ahn, K., Meyer, T. H., Uebel, S., Sempé, P., Djaballah, H., Yang, Y., Peterson, P. A., Früh, K., and Tampé, R. (1996) *EMBO J.* **15,** 3247–3255
35. Alberts, P., Daumke, O., Deverson, E. V., Howard, J. C., and Knittler, M. R. (2001) *Curr. Biol.* **11,** 242–251
36. Maruta, S., Henry, G. D., Sykes, B. D., and Ikebe, M. (1993) *J. Biol. Chem.* **268,** 7093–7100
37. Sauna, Z. E., Smith, M. M., Müller, M., and Ambudkar, S. V. (2001) *J. Biol. Chem.* **276,** 21199–21208
38. Werber, M. M., Peyser, Y. M., and Muhlrad, A. (1992) *Biochemistry* **31,** 7190–7197
39. Cai, J., Daoud, R., Alqawi, O., Georges, E., Pelletier, J., and Gros, P. (2002) *Biochemistry* **41,** 8058–8067
40. Sauna, Z. E., Smith, M. M., Muller, M., and Ambudkar, S. V. (2001) *J. Biol. Chem.* **276,** 33301–33304
41. Fisher, A. J., Smith, C. A., Thoden, J. B., Smith, R., Sutoh, K., Holden, H. M., and Rayment, I. (1995) *Biochemistry* **34,** 8960–8972
42. Gaudet, R., and Wiley, D. C. (2001) *EMBO J.* **20,** 4964–4972
43. Smith, P. C., Karpowich, N., Millen, L., Moody, J. E., Rosen, J., Thomas, P. J., and Hunt, J. F. (2002) *Mol. Cell* **10,** 139–149
44. Hopfner, K. P., Karcher, A., Shin, D. S., Craig, L., Arthur, L. M., Carney, J. P., and Tainer, J. A. (2000) *Cell* **101,** 789–800
45. Locher, K. P., Lee, A. T., and Rees, D. C. (2002) *Science* **296,** 1091–1098
46. Lapinski, P. E., Raghuraman, G., and Raghavan, M. (2003) *J. Biol. Chem.* **278,** 8229–8237
47. Hung, L. W., Wang, I. X., Nikaido, K., Liu, P. Q., Ames, G. F., and Kim, S. H. (1998) *Nature* **396,** 703–707
48. Sankaran, B., Bhagat, S., and Senior, A. E. (1997) *FEBS Lett.* **417,** 119–122
49. Senior, A. E., and Bhagat, S. (1998) *Biochemistry* **37,** 831–836
50. Liu, C. E., Liu, P. Q., and Ames, G. F. (1997) *J. Biol. Chem.* **272,** 21883–21891
51. Davidson, A. L., and Sharma, S. (1997) *J. Bacteriol.* **179,** 5458–5464
52. Szabo, K., Szakacs, G., Hegeds, T., and Sarkadi, B. (1999) *J. Biol. Chem.* **274,** 12209–12212
53. Chen, J., Sharma, S., Quiocho, F. A., and Davidson, A. L. (2001) *Proc. Natl. Acad. Sci. U. S. A.* **98,** 1525–1530
54. Qu, Q., Russell, P. L., and Sharom, F. J. (2003) *Biochemistry* **42,** 1170–1177
55. Sauna, Z. E., and Ambudkar, S. V. (2000) *Proc. Natl. Acad. Sci. U. S. A.* **97,** 2515–2520
56. van Veen, H. W., Margolles, A., Muller, M., Higgins, C. F., and Konings, W. N. (2000) *EMBO J.* **19,** 2503–2514
57. Janas, E., Hofacker, M., Chen, M., Gompf, S., van der Does, C., and Tampé, R. (2003) *J. Biol. Chem.* **278,** 26862–26869